Journal of the Taiwan Institute of Chemical Engineers 50 (2015) 297–305

Contents lists available at ScienceDirect

Journal of the Taiwan Institute of Chemical Engineers

journal homepage: www.elsevier.com/locate/jtice

Synthesis and characterization of green agents coated Pd/Fe bimetallic nanoparticles

Xiangyu Wang [a,*], Lan Le [a], Pedro J.J. Alvarez [b], Fang Li [a], Kunqian Liu [a]

[a] Faculty of Environmental Science and Engineering, Kunming University of Science and Technology, Kunming 650500, China
[b] Department of Civil and Environmental Engineering, Rice University, Houston, TX 77005, USA

ARTICLE INFO

Article history:
Received 11 June 2014
Revised 19 November 2014
Accepted 28 December 2014
Available online 19 January 2015

Keywords:
Pd/Fe NPs
Modification
Dispersity
Dechlorination
2,4-Dichlorophenol

ABSTRACT

The low stability and mobility of nanoparticles in liquid phase is one of the biggest challenges for the application of zero-valent iron (ZVI) technology. In this research, three green agents, polyethylene glycol (PEG), starch, and guar gum were coated on Pd/Fe bimetallic nanoparticles (NPs) to enhance the stability and reactivity of Pd/Fe NPs. The modified NPs (PEG-Pd/Fe, Starch-Pd/Fe, and Guar gum-Pd/Fe NPs) were characterized in terms of specific surface area, particle size, shape, morphology, and structural feature, *etc.* The results show that the diameters of modified Pd/Fe NPs are in the range of 60–100 nm. Compared with the pristine unmodified Pd/Fe NPs, the aggregations of modified Pd/Fe NPs were successfully reduced. XRD patterns indicate that modified Pd/Fe NPs remained the body centered cubic crystal structure, and the modification process contributed to improve the antioxidant ability. 2,4-Dichlorophenol (2,4-DCP) dechlorination experiments show that physico-chemical properties of the three modifiers have different effects on the reactivity of modified Pd/Fe NPs. The initial pH value of the reaction system had complex effects on the dechlorination of 2,4-DCP by using modified Pd/Fe NPs. Activation energies of pristine, PEG-Pd/Fe, Starch-Pd/Fe, and Guar gum-Pd/Fe NPs were calculated to be 39.47 kJ/mol, 38.66 kJ/mol, 36.59 kJ/mol, and 33.88 kJ/mol, respectively, implying that the modification process can enhance the dechlorination rate of Pd/Fe NPs, and that catalytic hydrodechlorination process of 2,4-DCP with modified Pd/Fe NPs is a surface-controlled chemical reaction.

1. Introduction

Nanoscale zero valent iron (nZVI) particles have attracted a widespread attention because of their unique properties, such as large surface area, high reactivity, and low cost. Recently, nZVI has widely been applied in wastewater treatment and soil/groundwater decontamination. NZVI technology has already shown outstanding environmental remediation capacity, especially in dechlorination of chlorinated organic compounds (COCs) [1-8], decolorization of dye waste [9-13], sequestration of heavy metals [14-19], and reduction of inorganic anions [20-23], *etc.* As a strong reductant, nZVI has the following advantages for practical subsurface remediation, compared with their bulk or micro counterparts: (1) nZVI has smaller particle size and larger specific surface area, resulting in higher chemical reactivity; (2) dechlorination efficiency and reaction rate of many COCs (such as trichloroethylene) with nZVI can be enhanced so as to avoid the formation of toxic intermediates produced from incomplete dechlorination [24]; (3) the nano size of nZVI makes it possible to mobile sufficiently within porous structures of deep subsurface environments. In addition, nZVI has gained its second life by coating a layer of second metal onto the surface of Fe^0 to form bimetallic particles (including Pd/Fe [1,2,4,5], Ni/Fe [25-27], Pt/Fe [28], and Cu/Fe [29] bimetallic NPs, *etc.*). Therefore, a rapid and complete dechlorination can be achieved comparing with monometallic Fe^0.

Currently, nZVI are prepared by the redox reaction between Fe^{2+} or Fe^{3+} ions and reductants (such as sodium borohydride, and potassium borohydride) in aqueous solution. Iron based bimetallic nanoparticles are prepared by either depositing Pd on the surface of nZVI or reducing iron ions and second metal cations with sodium borohydride/potassium borohydride simultaneously [30]. Although the aforementioned preparation method is simple and can be safely conducted in chemistry laboratory [8], the freshly prepared NPs are prone to aggregate each other, thus decrease nZVI's stability, mobility, and longevity under subsurface environments, resulting in the limitation of the full-scale field application of nZVI technology. An effective method for increasing the dispersity of nZVI in liquid phase is surface modification with surfactants [31] or/and coatings with polyelectrolyte [6,7,32-35].

Theoretically, modification or coating agents used for reducing the aggregation of NPs are expected to meet the following

* Corresponding author. Tel.: +86 87165170906.
E-mail address: imusthlee2014@sina.com (X. Wang).

http://dx.doi.org/10.1016/j.jtice.2014.12.030
1876-1070/

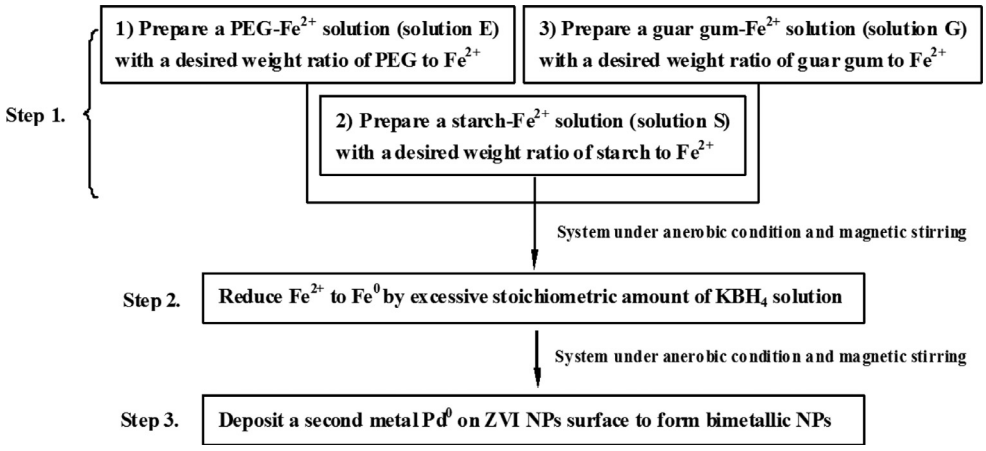

Fig. 1. Schematic of synthesis procedure of three green agents modified Pd/Fe NPs.

requirements: (1) low-toxicity, (2) inexpensiveness, (3) water-solubility, (4) biodegradability, and (5) more importantly, capability of stabilizing nZVI in aqueous solution for *in situ* environmental remediation. Therefore, three green agents, PEG (200), starch, and guar gum, are chosen in this study for modification of nZVI. PEG (200), starch, and guar gum have commonly been used as a food additive. The three green agents, especially guar gum, contain a large number of hydroxyl groups in their molecules structure that are able to adsorb Fe nanoparticles, thus prevent the agglomeration of nZVI in aqueous solution. The objective of this research is to provide an effective method for preparation of modified nZVI or iron based bimetallic nanoparticles with enhanced stability in liquid phase and decreased degree of aggregation by using environment-friendly agents. Even though a variety of chemical agents have been reported for modification of Pd/Fe or Fe NPs, to the best of our knowledge, there is little available information about the effects of modification and synthesis conditions of PEG (200), starch, and guar gum on dechlorination effectiveness of Pd/Fe NPs. Moreover, the effects of pH value on dechlorination ability of the modified Pd/Fe NPs are not well-documented. 2,4-Dichlorophenol (2,4-DCP), a typical chlorinated organic pollutant, was target pollutant in this study. 2,4-DCP has been widely used as solvent, pesticide, and pharmaceutical intermediate for decades, and caused great concern due to its toxicity. Once released into the ground water or soil, it will accumulate and can be hardly biodegradated in water ecosystems, thus endangers the health of humans [36]. However, through effective dehalogenation, 2,4-DCP can be degradated into less toxic and more biodegradable products, such as 2-chlorophenol (2-CP), 4-chlorophenol (4-CP), and phenol (P). The further objective of this study is to assess the dechlorination efficiency of 2,4-DCP with the three green agents modified Pd/Fe NPs in aqueous solution. For better understanding of dechlorination mechanism, dechlorination activation energies and kinetics of pristine and modified Pd/Fe NPs were also investigated.

2. Experimental section

2.1. Materials

Ferrous sulphate heptahydrate ($FeSO_4{\cdot}7H_2O$), potassium borohydride (KBH_4), polyethylene glycol (PEG, $M_W = 200$), starch, ethanol, acetone, and guar gum were purchased from Kermel (Tianjin, China), 2,4-dichlorophenol (2,4-DCP), 4-chlorophenol (4-CP), 2-chlorophenol (2-CP), and phenol (P) from Ourchem (Sinopharm Chemical Reagent Co. Ltd.), and palladium acetate ($[Pd(C_2H_3O_2)_2]_3$) from Aldrich. All chemicals were of reagent grade, and used as received.

2.2. Preparation of Pd/Fe bimetallic NPs

The preparation process for Pd/Fe bimetallic NPs was carried out in an anaerobic chamber. 1 M solution of Fe^{2+} was firstly prepared by dissolving $FeSO_4{\cdot}7H_2O$ in deionized water (200 mL). Then a given amount of PEG or guar gum was added to produce a solution (hereafter denoted the obtained solutions as solution E and G, respectively) that could be mixed by magnetic stirring. Meanwhile, a 200 mL starch solution with a certain concentration was obtained by dissolving starch in boiling water, and 0.2 mol $FeSO_4{\cdot}7H_2O$ was then added into the solution to produce solution S. Separately, a solution of 0.8 mol KBH_4 (200 mL) was added into a 250 mL bottle. The solution E, G, and S were then placed on a magnetic stirrer. The reaction was initiated by dropwise excess KBH_4 solution into Fe^{2+} solution. The reduction of Fe^{2+} was not completed until all the KBH_4 solution was dropwised, resulting in the formation of black-colored nZVI. The freshly prepared nZVI was washed with 200 mL deionized water and absolute ethanol for three times, respectively, followed by soaking the modified nZVI particles into an ethanol solution of palladium acetate under magnetic stirring for 30 min, resulting in the deposition of Pd^0 on ZVI NPs surface. Three modified bimetallic NPs with PEG, starch and guar gum were referred to hereafter as E-Pd/Fe, S-Pd/Fe, and G-Pd/Fe NPs, respectively. For comparison, unmodified Pd/Fe NPs were prepared by using the similar synthesis procedure, except that no modifier was added into the reaction solution. Nitrogen gas was continuously flowed in an effort to prevent the oxidation of freshly prepared NPs (Fig. 1).

2.3. Characterization of Pd/Fe bimetallic NPs

BET (Brunauer–Emmett–Teller) specific surface areas (SSA) of dried Pd/Fe NPs had been measured by means of N_2 adsorption/desorption isotherms with a TriStar II 3020 V1.03 analyzer (Micromeritics Instrument Corporation). To determine the relative surface area, the modified Pd/Fe NPs were dissolved in deionized water and added into a particle surface area analyzer (Xigo Nanotools Acorn Area). X-ray diffractometer (XRD) patterns of modified and unmodified Pd/Fe NPs were collected on a D/max2200 (Rigaku Corp., Japan) using Ni-filtered Cu Kα radiation operating at an accelerating voltage of 45 kV and emission current of 40 mA ($\lambda = 0.15418$ nm) in a step scanning mode, with a step size of 0.02, and a counting time of 1 s per step in the range 10–90. The intermolecular distance d was calculated using Bragg's first-order X-ray diffraction equation ($d = \lambda/(2 \sin \theta)$). Field emission scanning electron microscope (FE-SEM) pictures were collected on a high-resolution JSM-6700F (FESEM, JEOL Ltd., Japan) to observe the morphology of NPs. All samples were sprayed with a

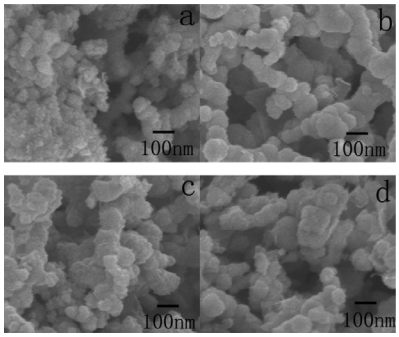

Fig. 2. SEM images of Pd/Fe NPs: (a) pristine Pd/Fe NPs, (b) PEG-Pd/Fe NPs, (c) Starch-Pd/Fe NPs, and (d) Guar gum-Pd/Fe NPs.

thin layer of gold for 1 min before being scanned for all cases. Transmission electron microscope (TEM) images were obtained on a JEM 1200EX transmission electron microscope (TEM, JEOL Ltd., Japan) at an acceleration voltage of 100 kV to reveal particle shape, diameter, and size distribution of NPs. Pd/Fe NPs were ultrasonicated in acetone, followed by dropping the resulting suspension on a 300-mesh gold/copper lacey carbon grid before visualization under TEM.

2.4. Dechlorination experiments

For each dechlorination reaction, a certain amount of modified Pd/Fe NPs and 100 mL of 2,4-DCP with an initial concentration of 20 mg/L were both added to a 250 mL volume serum bottle, followed by sealing the bottle with Teflon-lined rubber septums immediately. The bottles were then placed into a temperature-controlled orbital shaker with a constant shaking rate of 170 rpm. Contrast experiments were conducted with the same amount of unmodified Pd/Fe NPs under the identical reaction condition. In addition, control experiments (without the addition of the NPs) were carried out in parallel. At selected time intervals, 5 mL of the aqueous sample was withdrawn for the analysis of 2,4-DCP dechlorination efficiency. The solution in the sampler was filtered through a 0.45 μm filters prior to subsequent analyses. All experimental points were triplicated.

The concentrations of the target pollutant (2,4-DCP), dechlorination intermediates (*i.e.* 2-CP and 4-CP), and final product (phenol) were measured with a 1260 HPLC (Agilent) equipped with an UV–vis detector. The wavelength of the detector was set at 283 nm. A mixture of methanol and water (60:40, v/v) was used as an eluent, and the flow rate was 1.0 mL/min. The size of the sample loop was 10 μL.

3. Results and discussion

3.1. Characterization of Pd/Fe bimetallic NPs

The surface morphologies of unmodified and modified Pd/Fe NPs are shown in Fig. 2. Pristine Pd/Fe NPs are highly conglomerated with a rough surface morphology, and Fig. 2a shows that unmodified Pd/Fe NPs are with severe aggregation due to magnetic force between iron NPs. In contrast, the modified Pd/Fe NPs are with spherical shape, and a particle size ranges from 60 nm to 100 nm. Notably, the aggregation of modified Pd/Fe NPs was significantly decreased, indicating that the modifiers played an important role in increasing the dispersity of NPs. The particle sizes of S-Pd/Fe and G-Pd/Fe NPs were slightly larger than that of E-Pd/Fe NPs. This phenomenon is in agreement with the measurement of the specific surface area (SSA). The SSA of E-Pd/Fe, S-Pd/Fe, and G-Pd/Fe NPs were 44.6 m^2/g, 32.1 m^2/g, and 30.8 m^2/g, respectively. In order to have a further understanding of the particle size and dispersiveness of the modified Pd/Fe NPs in liquid phase, the relative surface areas of NPs in solution were measured and the results are shown in Fig. 3. The relative surface areas of modified Pd/Fe

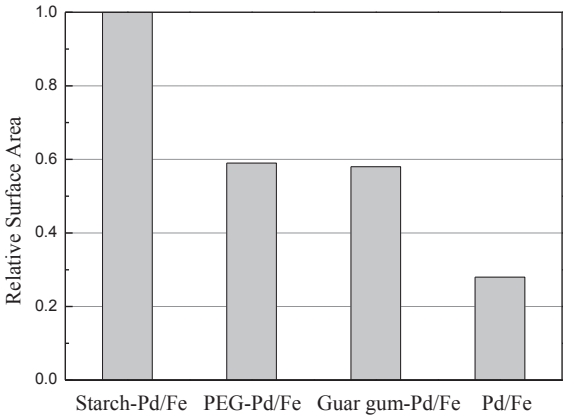

Fig. 3. Relative surface area of modified Pd/Fe NPs and pristine Pd/Fe NPs measured in solution.

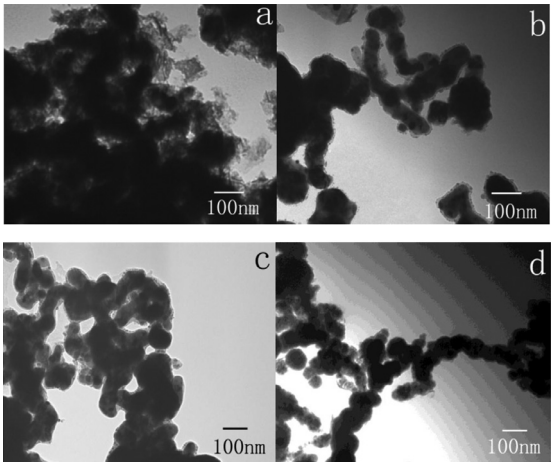

Fig. 4. TEM images of Pd/Fe NPs: (a) pristine Pd/Fe NPs, (b) PEG-Pd/Fe NPs, (c) Starch-Pd/Fe NPs, and (d) Guar gum-Pd/Fe NPs.

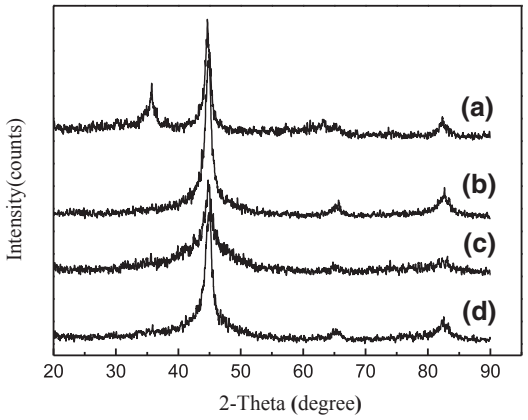

Fig. 5. XRD patterns of Pd/Fe NPs: (a) unmodified Pd/Fe NPs, (b) Guar gum-Pd/Fe NPs, (c) Starch-Pd/Fe NPs, and (d) PEG-Pd/Fe NPs.

NPs are larger than that of the pristine Pd/Fe NPs, indicating that, by coating with the three green agents, the dispersity of modified Pd/Fe NPs had been dramatically increased in liquid phase.

Fig. 4 presents the TEM images of the pristine and modified Pd/Fe NPs. Fig. 4a shows an unclear outline of unmodified Pd/Fe NPs and serious agglomeration. This observation result is consistent with that shown in SEM images. By contrast, the outlines of the majority of modified Pd/Fe NPs can be distinguished from each other. This implies

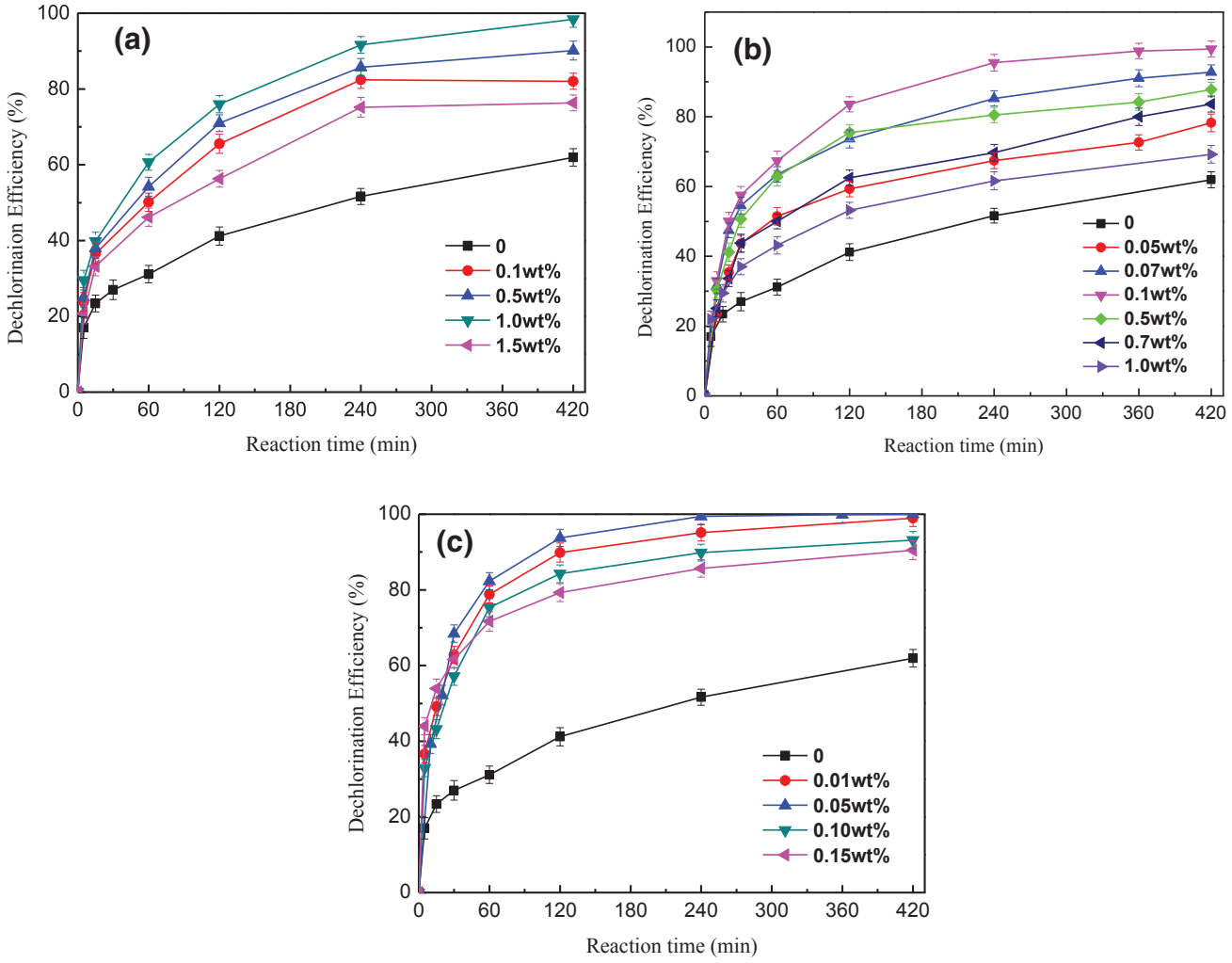

Fig. 6. Effect of modifier concentration on 2,4-DCP dechlorination efficiency: (a) PEG-Pd/Fe NPs, (b) Starch-Pd/Fe NPs, and (c) Guar gum-Pd/Fe NPs (C_0 = 20 mg/L, $\rho_{Pd/Fe}$ = 10 g/L initial pH 7.0, T = 20 °C).

that, compared with pristine Pd/Fe NPs, the aggregation of modified Pd/Fe NPs had been greatly reduced.

The crystal structures of pristine and modified Pd/Fe NPs were examined with XRD, and the results are shown in Fig. 5. The distinct Fe^0 peaks of modified Pd/Fe NPs (2θ = 44.80°, 64.78°, and 82.63°) could be observed, indicating the crystal structure of Pd/Fe NPs is of a regular bcc α-Fe crystalline state. But for pristine Pd/Fe NPs, another peak at 34.9° was observed, suggesting that the Pd/Fe NPs prepared without the coating of modifiers had been oxidized. Therefore, it might be concluded that the coating of the three green agents contributed to the increase in antioxidant capacity of modified Pd/Fe NPs.

3.2. Dechlorination reactivity of modified Pd/Fe NPs

3.2.1. Effect of dispersant concentration

The effects of PEG, starch, and guar gum concentrations on the removal of 2,4-DCP with modified Pd/Fe NPs are shown in Fig. 6. Dechlorination experiments were conducted at a 20 mg/L initial concentration of 2,4-DCP for 420 min. Compared with unmodified Pd/Fe NPs, 2,4-DCP dechlorination efficiencies were increased with modified Pd/Fe NPs. 2,4-DCP dechlorination efficiencies were affected by different concentrations of PEG, starch, and guar gum. The dechlorination efficiency of 2,4-DCP with E-Pd/Fe NPs increased with increasing the concentration of PEG when it was lower than 1.0 wt%, while the trend reversed with the concentration higher than 1.0 wt%,

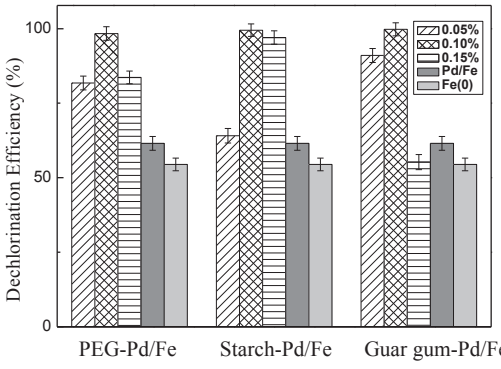

Fig. 7. Effect of Pd content of modified Pd/Fe NPs on 2,4-DCP dechlorination efficiency (C_0 = 20 mg/L, $\rho_{Pd/Fe}$ = 10 g/L initial pH 7.0, T = 20 °C, reaction time = 420 min).

indicating the optimal PEG concentration could be 1.0 wt%. At a PEG concentration larger than 1.0 wt%, the excess amount of hydroxyl groups of PEG might bind more water by hydrogen bonds, which did not facilitate the dispersion of NPs. For the case of S-Pd/Fe NPs, the dechlorination efficiency of 2,4-DCP was increased with the increase of the starch concentration when it was lower than 0.1 wt%. However, the dechlorination efficiency was decreased with the increase of the starch concentration when it was higher than 0.1 wt%.

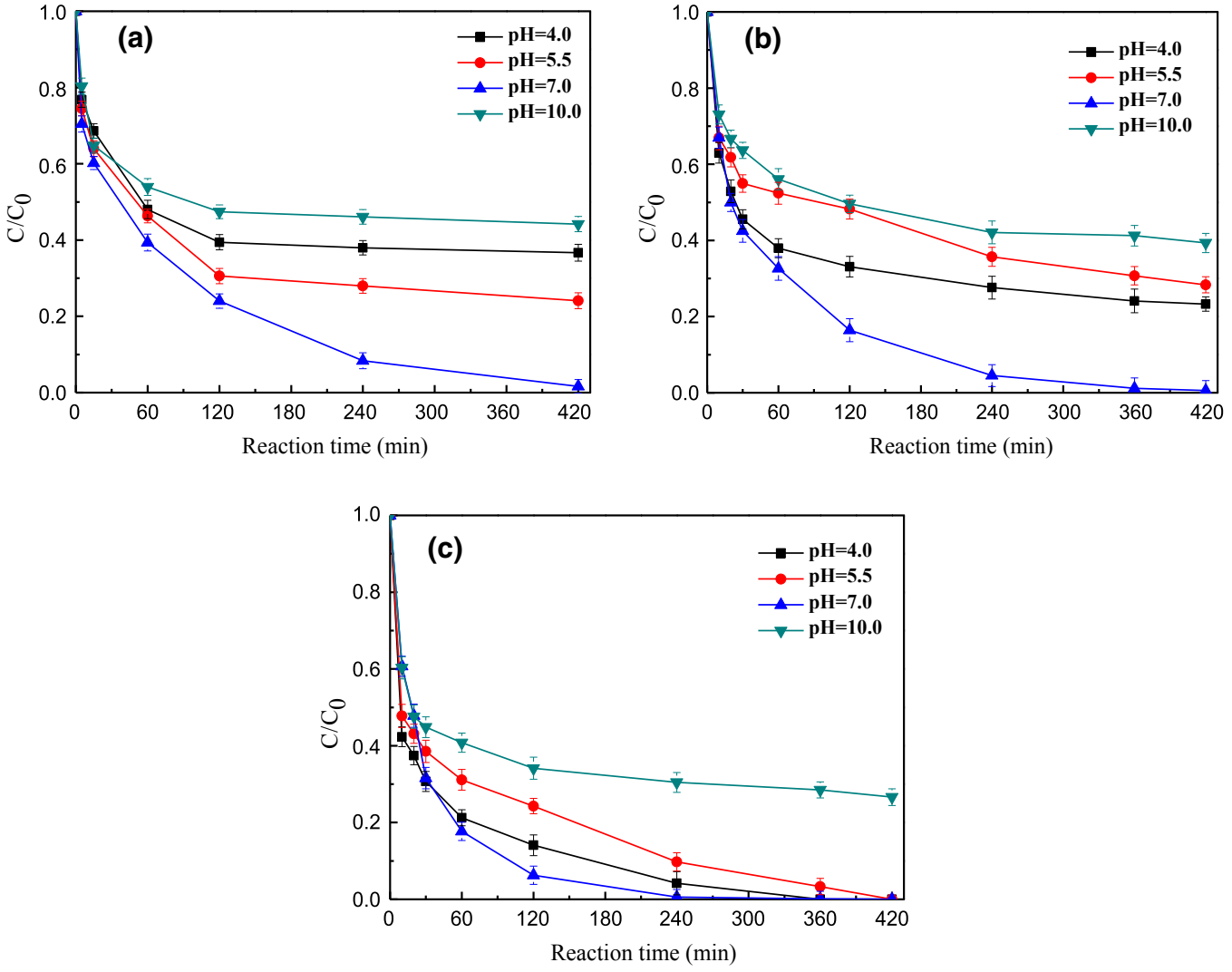

Fig. 8. Effect of initial pH value on 2,4-DCP dechlorination efficiency with modified Pd/Fe NPs: (a) PEG-Pd/Fe NPs (PEG addition = 1.0 wt%), (b) Starch-Pd/Fe NPs (starch addition = 0.1 wt%), and (c) Guar gum-Pd/Fe NPs (guar gum addition = 0.05 wt%, C_0 = 20 mg/L, $\rho_{Pd/Fe}$ = 10 g/L , T = 20 °C, Pd content = 0.1 wt%).

Hence, the starch concentration could be optimized to 0.1 wt%. When the starch concentration was not as high as 0.1 wt%, the starch coated on NPs was still less than enough, thus the dechlorination efficiency was not able to be the maximum value. At a concentration higher than 0.1 wt%, the thick coating layers of starch played a negative role that blocked the contact of target pollutant and Pd/Fe NPs. From Fig. 6c, the highest 2,4-DCP dechlorination efficiency with G-Pd/Fe NPs had been achieved at a guar gum concentration of 0.05 wt%. This is because that guar gum is a nonionic water soluble polysaccharide with each unit containing nine hydroxyl groups. The hydroxyl groups in guar gum are available for bonding Fe^{2+}, thus contributing to preparing Pd/Fe NPs with better dispersity. However, with guar gum concentration higher than 0.05 wt%, the reactive sites on surface of Pd/Fe NPs might be covered by the coating of guar gum. It is noteworthy that 2,4-DCP dechlorination efficiencies with G-Pd/Fe NPs are higher than that of E-Pd/Fe and S-Pd/Fe NPs. At optimized concentration of modifiers, the dechlorination efficiencies with different modified Pd/Fe NPs followed the orders of G-Pd/Fe> S-Pd/Fe > E-Pd/Fe. The possible explanation of this tendency is due to that guar gum and starch have more hydroxyl groups than PEG. In the following dechlorination experiments, the concentrations of guar gum, starch, and PEG for preparation of modified Pd/Fe NPs were set at 0.05 wt%, 0.1 wt% and 1.0 wt%, respectively.

3.2.2. *Effect of Pd content*

In the catalytic dechlorination reaction between 2,4-DCP and Pd/Fe NPs, Fe is considered as a reductant to produce H_2 by its corrosion in water, while Pd nanoparticle as a catalyst to activate H_2 on the surface of NPs. It was reported that the Pd-H* was formed due to the dissociation of H_2 on the Pd surface when molecular hydrogen was provided. The produced hydrogen species catalyzed the dechlorination of chlorinated organic compounds (Eqs. (1) and (2)) [37].

$$Pd^0 + H_2 \rightarrow Pd \bullet 2H^* \quad (1)$$

$$Pd \bullet 2H^* + Pd \bullet Cl \bullet R \rightarrow RH + H^+ + Cl^- + 2Pd^0 \quad (2)$$

Such catalytic reduction system is anticipated to have higher dechlorination reactivity compared with monometallic Fe NPs. Thus Pd content can be regarded as an important factor which greatly affects the dechlorination ability of Pd/Fe NPs. Previous studies reported that there existed an optimum Pd content of Pd/Fe bimetallic NPs [38-40]. In this study, the effect of Pd contents (weight ratio of Pd to Fe NPs) ranged from 0.05% to 0.15% on 2,4-DCP dechlorination efficiency was investigated (Fig. 7). 2,4-DCP dechlorination efficiencies with E-Pd/Fe, S-Pd/Fe, and G-Pd/Fe NPs are higher than that of unmodified Pd/Fe or Fe NPs. The lower 2,4-DCP dechlorination efficiency

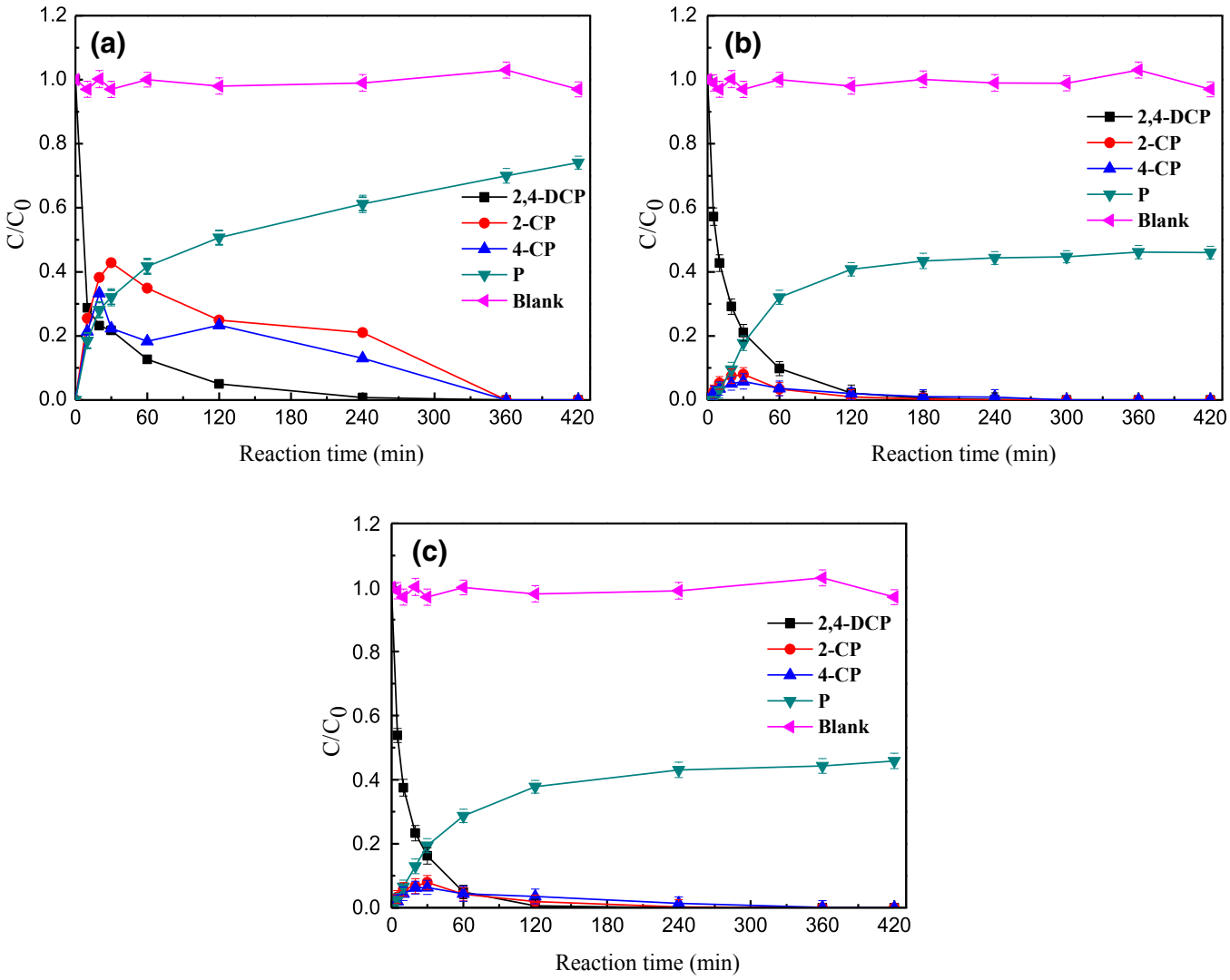

Fig. 9. Catalytic dechlorination of 2,4-DCP with modified Pd/Fe NPs: (a) PEG-Pd/Fe NPs, $T = 30$ °C, Pd content = 0.1 wt%; (b) Starch-Pd/Fe NPs, $T = 20$ °C, Pd content = 0.15 wt%; and (c) Guar gum-Pd/Fe NPs, $T = 35$ °C, Pd% = 0.1 wt % ($C_0 = 20$ mg/L, $\rho_{Pd/Fe} = 10$ g/L , initial pH 7.0).

with pristine Pd/Fe NPs can be ascribed to both the aggregation of NPs and decrease in surface area.

As shown in Fig. 7, with increasing the Pd contents of E-Pd/Fe, S-Pd/Fe, and G-Pd/Fe NPs at Pd content <0.1%, the corresponding 2,4-DCP dechlorination efficiencies were increased because of the increase in reactive hydrogen species (Pd-H*) on the surface of Pd/Fe NPs. With the Pd contents of modified Pd/Fe NPs >0.1%, dechlorination efficiency was decreased with the increase of Pd content. The most likely explanation for the decrease of dechlorination efficiency at Pd content >0.1% is due to the fact that accumulation of excessive hydrogen gas adsorbed on the surface of Pd hindered the available reactive sites of modified Pd/Fe NPs for dechlorination of target pollutant [40], thus resulting in the decrease in dechlorination efficiency. This result was in accordance with a previous study in which the optimized Pd content of unmodified Pd/Fe NPs was reported to be 0.1% for MCAA dechlorination [41]. Therefore, 0.1% Pd content was chosen as optimum Pd content of E-Pd/Fe, S-Pd/Fe, and G-Pd/Fe NPs for the subsequent dechlorination experiments.

3.2.3. Effect of pH

For catalytic dechlorination of COCs with Pd/Fe NPs, Pd on the surface of nZVI acts as a collector of active hydrogen species (Pd-H*) resulted from iron corrosion. Thus, the initial pH value of the reaction system is supposed to have effect on dechlorination efficiency. As shown in Fig. 8, the highest dechlorination efficiency was obtained at pH 7, while the lowest dechlorination efficacy at pH 10 for the modified Pd/Fe NPs. This result is not totally consistent with the previous experimental results that dechlorination efficiency was increased with the decrease of pH value [42]. It is also worth noting that the pH value of 7 under which the highest 2,4-DCP dechlorination efficiency was obtained was close to the value of p*K*a of 2,4-DCP (7.8). A reasonable explanation for these results was that the certain properties of 2,4-DCP in aqueous solution changed the influence of pH on the corrosion of nZVI, thus leading to the content variation of active hydrogen species (Pd-H*) on the surface of Pd and exhibiting complex effects of pH on 2,4-DCP dechlorination efficiency. In short, such a complicated effect of pH on 2,4-DCP dechlorination efficiency was the result of a combined impacts between the physic-chemical properties of target pollutant and modifiers, coupling with their surrounding environmental conditions.

3.3. Reactive mechanism and kinetics for 2,4-DCP dechlorination

The intermediates and final products of 2,4-DCP dechlorination with modified Pd/Fe NPs were analyzed to investigate the dechlorination mechanism. As shown in Fig. 9, almost all 2,4-DCP was

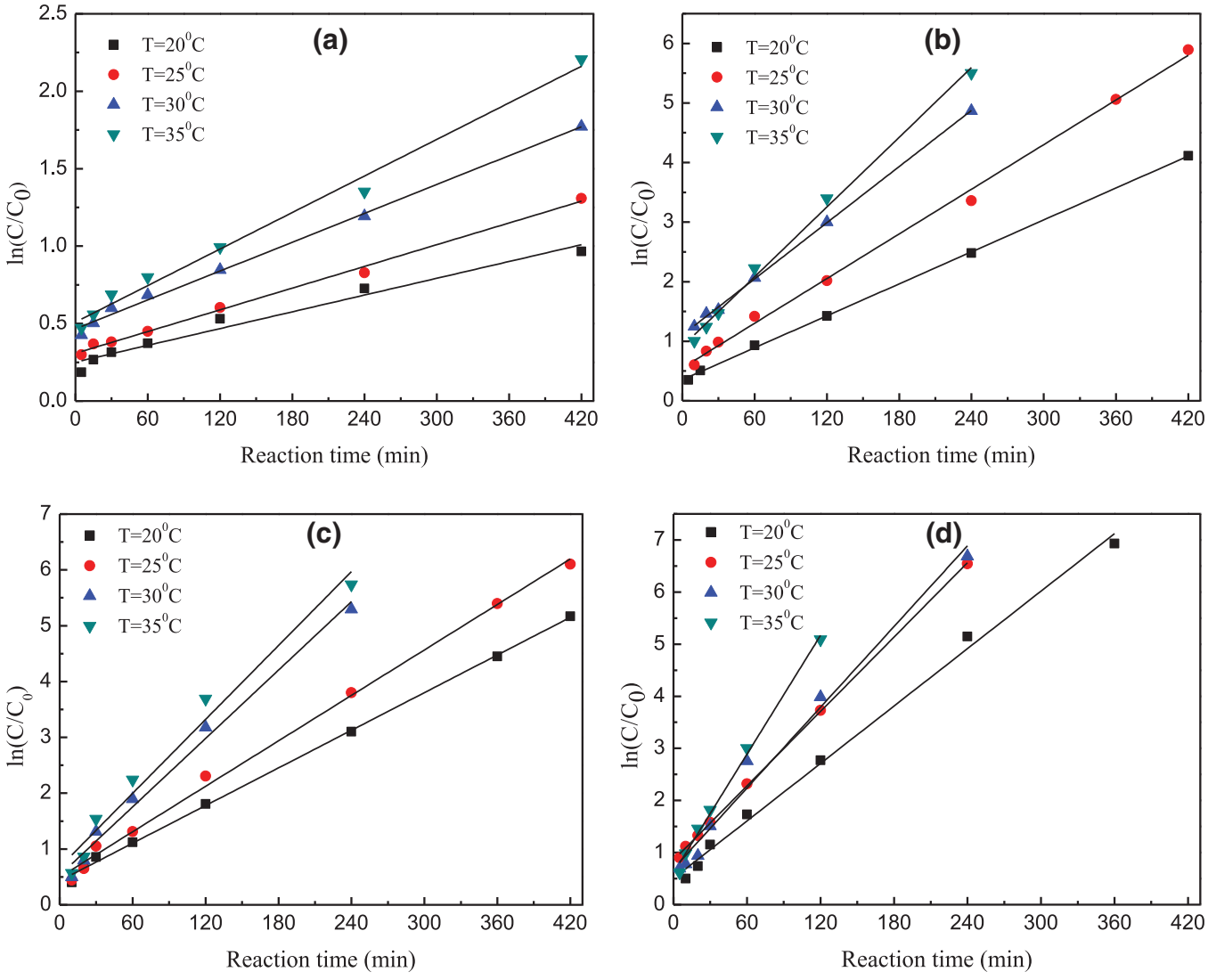

Fig. 10. Dechlorination of 2,4-DCP by modified Pd/Fe NPs at different temperatures. (a) Pristine Pd/Fe, (b) PEG-Pd/Fe NPs, (c) Starch-Pd/Fe NPs, and (d) Guar gum-Pd/Fe NPs ($C_0 = 20$ mg/L, $\rho_{Pd/Fe} = 10$ g/L , initial pH 7.0, Pd content = 0.1 wt%).

dechlorinated by modified Pd/Fe NPs within 300 min, while the concentration of the final dechlorination product phenol was increased as time continued, together with the yield of the intermediates 2-CP and 4-CP. In the beginning of the reaction, the concentrations of 2-CP and 4-CP increased promptly, and afterwards decreased steadily after 30 min, indicating 2-CP and 4-CP could be further degradated via sequential hydrogenolysis. As shown in Fig. 9a–c, both the concentration and the yielding rate of 2-CP are higher than that of 4-CP, illustrating that 2-CP could be more easily dechlorinated than 4-CP. It is worthwhile to note that phenol was identified immediately as soon as the dechlorination reaction was conducted. This proves that the catalytic dechlorination of 2,4-DCP with modified Pd/Fe NPs is a multistep reaction. Accompanied with the stepwise dechlorination, 2,4-DCP could be directly removed into phenol. It can be concluded that the possible 2,4-DCP dechlorination pathway with modified Pd/Fe NPs includes the following steps: (1) the diffusion of 2,4-DCP in aqueous solution into the surface of modified Pd/Fe NPs; (2) the adsorption of 2,4-DCP onto the surface of modified Pd/Fe NPs; (3) the dechlorination process of 2,4-DCP and the formation of intermediate and final products on the surface of modified Pd/Fe NPs; (4) the desorption of products formed on the surface of Pd/Fe NPs after dechlorination of 2,4-DCP; and (5) the diffusion of the resulted final products into aqueous solution. However, the total concentration of phenol was smaller than the initial concentration of 2,4-DCP after 2,4-DCP was completely dechlorinated. On one hand, this was probably due to the partly volatilization of phenol in aqueous solution; on the other hand, this was attributed to adsorption of phenol by Fe^{2+} resulted from Fe^0 NPs corrosion or the chemical reaction between phenol and Fe^{3+} formed from the oxidation process of Fe^{2+} in aqueous solution [43].

Previous studies on dechlorination process of COCs using Fe NPs or their bimetallic counterparts have shown that dechlorination kinetics could be expressed as a pseudo-first-order reaction [44]. The reaction rate equation for the disappearance of 2,4-DCP in the dechlorination system is shown as follows:

$$v = -\frac{dC_{2,4-DCP}}{dt} = k_{SA}\alpha_s\rho_m C_{2,4-DCP} = k_{obs}C_{2,4-DCP} \quad (3)$$

$$\ln\left(\frac{C_{2,4-DCP}}{C_{2,4-DCP,0}}\right) = -k_{obs}t \quad (4)$$

where $C_{2,4\text{-DCP}}$ is the 2,4-DCP concentration (mg/L), $C_{2,4\text{-DCP},0}$ is the initial 2,4-DCP concentration (mg/L), k_{obs} is the observed reaction rate constant for a pseudo-first-order reaction (min^{-1}) and can be calculated from Eq. (4), k_{SA} is the specific reaction rate constant (L/min m^2),

Table 1
Observed reaction rate constant of 2,4-DCP dechlorination by modified Pd/Fe NPs at different temperatures.[a]

Temperature (°C)	PEG-Pd/Fe		Starch-Pd/Fe		Guar gum-Pd/Fe	
	k_{obs}	R^2	k_{obs}	R^2	k_{obs}	R^2
20	0.89×10^{-2}	0.9994	1.12×10^{-2}	0.9984	1.84×10^{-2}	0.9942
25	1.25×10^{-2}	0.9972	1.36×10^{-2}	0.9960	2.38×10^{-2}	0.9996
30	1.57×10^{-2}	0.9993	2.04×10^{-2}	0.9861	2.58×10^{-2}	0.9810
35	1.95×10^{-2}	0.9944	2.21×10^{-2}	0.9702	3.80×10^{-2}	0.9941

[a] The initial concentration of 2,4-DCP was 20 mg/L and the reaction time was 420 min.

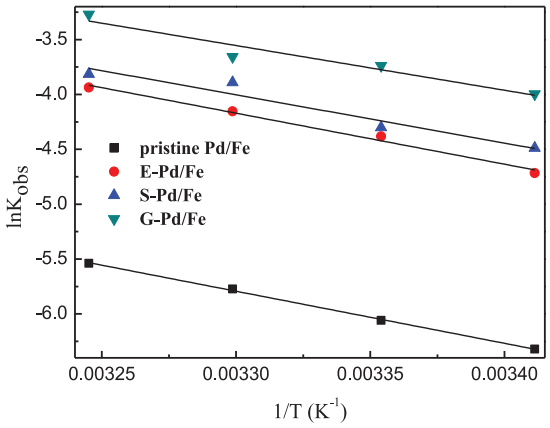

Fig. 11. Arrhenius plot for the estimation of activation energy: 2,4-DCP dechlorination by modified Pd/Fe NPs.

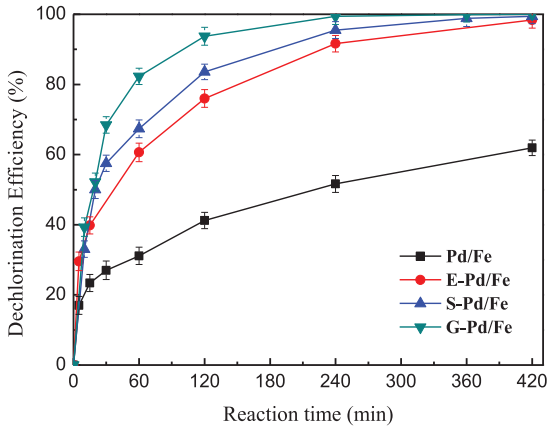

Fig. 12. Catalytic dechlorination of 2,4-DCP with Pd/Fe NPs: unmodified Pd/Fe NPs,1.0 wt% PEG-Pd/Fe, 0.1 wt% Starch-Pd/Fe NPs, 0.05 wt% Guar gum-Pd/Fe NPs ($C_0 = 20$ mg/L, $\rho_{Pd/Fe} = 10$ g/L , initial pH 7.0, $T = 20$ °C).

α_s is the specific surface area (m^2/g), ρ_m is the mass concentration (g/L), and t is the reaction time (min).

In order to have in-depth understanding of the reactive process and kinetics, batch experiments of 2,4-DCP dechlorination was carried out under different temperatures (Fig. 10). Plots of $\ln(C_{2,4\text{-DCP}}/C_{2,4\text{-DCP},0})$ versus t during hydrochlorination process had higher linear correlations ($R^2 > 0.97$) within 20–35 °C, implying that the catalytic dechlorination reaction of 2,4-DCP using modified and pristine unmodified Pd/Fe NPs can be described as a pseudo-first-order model. These results were consistent with the reported conclusions when Pd/Fe NPs were used to dechlorinate COCs in aqueous solutions [37,45].

Investigating activation energy of a certain chemical reaction helps to reveal which step will control the whole reaction. Previous literature has shown that diffusion controlled reaction usually has relatively low activation energy (8–21 kJ/mol), while the surface-control reaction have relatively higher activation energy (>29 kJ/mol) [5]. Thus, influences of reaction temperature on hydrodechlorination had been examined to distinguish the rate-limiting step and the k_{obs} data obtained from the slope of the fitting line (Fig. 10) under different temperatures were summarized in Table 1. Here a manipulated Arrhenius equation was introduced to describe the relationship between the k_{obs} and temperature:

$$\ln k_{obs} = -\frac{E_a}{RT} + \ln A \quad (5)$$

where E_a is the activation energy (kJ/mol), A is a frequency factor, R is the ideal gas constant (kJ/mol K), and T is the reaction temperature (K). Therefore, a plot of ln k_{obs} versus $1/T$ will result in a linear correlation according to Eq. (5). Fig. 11 shows the plot of ln k_{obs} versus $1/T$ for 2,4-DCP catalytic dechlorination by Pd/Fe bimetallic NPs. The activation energies (gained from the slops(E_a/R)) of 2,4-DCP dechlorination by E-Pd/Fe, S-Pd/Fe, and G-Pd/Fe NPs were 38.66 kJ/mol, 36.59 kJ/mol, and 33.88 kJ/mol, respectively, suggesting that the 2,4-DCP catalytic dechlorination by modified Pd/Fe NPs can be considered as a surface controlled chemical reaction. These orders of activation energies further confirmed that the modified Pd/Fe NPs under optimum conditions had different dechlorination properties (Fig. 12). Conversely, the activation energy of 2,4-DCP dechlorination with free modified Pd/Fe NPs was 39.47 kJ/mol, indicating that the modification of Pd/Fe NPs using PEG, starch and guar gum result in a lower activation energy, and that a faster chemical process during the hydrodechlorination by Pd/Fe metallic NPs can be anticipated through Pd/Fe nanoparticle modification approach.

4. Conclusion

Surface modification via chemical bond of iron ion and hydroxyl groups is a crucial process to reduce aggregation of iron bimetallic NPs and obtain stable NPs. The study herein investigated the effects of three kinds of green modifiers (PEG, starch, and guar gum) and the preparation process on the agglomeration and dechlorination efficiency of modified Pd/Fe NPs. The obtained results are as follows:

(1) Modified Pd/Fe NPs with a size ranges from 60 nm to 100 nm were successfully prepared via chemical bond of iron ion and hydroxyl groups by using commercially available, low cost, and non-hazardous green modifiers, and the aggregation of modified Pd/Fe NPs had been reduced.
(2) Synthesizing conditions have effects on the dechlorination properties of modified Pd/Fe NPs. Influences of concentrations of the different modifiers on 2,4-DCP dechlorination efficiency differ from each other due to the properties of modifiers. Dechlorination experiments on impacts of Pd content on the chemical reactivity of Pd/Fe NPs showed that the optimum Pd content was 0.1% (weight ratio of Pd to Fe) for modified NPs.
(3) The initial pH value plays a significant role in 2,4-DCP dechlorination by using PEG, starch, or guar gum modified Pd/Fe NPs. Influenced by the amount of atomic hydrogen H* and the

property of modifiers, the effect of pH on 2,4-DCP dechlorination process with modified Pd/Fe NPs is complicated. The optimal initial pH value for 2,4-DCP dechlorination with modified Pd/Fe was 7.

(4) Activation energies of unmodified Pd/Fe NPs, PEG-Pd/Fe, Starch-Pd/Fe, and Guar gum-Pd/Fe NPs are calculated to be 39.47 kJ/mol, 38.66 kJ/mol, 36.59 kJ/mol, and 33.88 kJ/mol, respectively, implying that the dechlorination efficiency of Pd/Fe NPs can be improved by modification process and that catalytic hydrodechlorination process of 2,4-DCP with modified Pd/Fe NPs is a surface-controlled chemical reaction.

Acknowledgements

This research is supported by the National Nature Science Foundation of China (NSFC, No. 51368025, and No. 51068011), China Scholarship Council (CSC, No. 20105024) and Yunnan Training Program of Innovation and Entrepreneurship for Undergraduates (No. 201210674108).

References

[1] Shih Y, Chen M, Su Y. Pentachlorophenol reduction by Pd/Fe bimetallic nanoparticles: effects of copper, nickel, and ferric cations. Appl Catal B Environ 2011;105:24–9.
[2] Kustov LM, Finashina ED, Shuvalova EV, Tkachenko OP, Kirichenko OA. Pd–Fe nanoparticles stabilized by chitosan derivatives for perchloroethene dechlorination. Environ Int 2011;37:1044–52.
[3] Zhang M, He F, Zhao D, Hao X. Degradation of soil-sorbed trichloroethylene by stabilized zero valent iron nanoparticles: effects of sorption, surfactants, and natural organic matter. Water Res 2011;45:2401–14.
[4] Zhang Z, Shen Q, Cissoko N, Wo J, Xu X. Catalytic dechlorination of 2,4-dichlorophenol by Pd/Fe bimetallic nanoparticles in the presence of humic acid. J Hazard Mater 2010;182:252–8.
[5] Lien H, Zhang W. Nanoscale Pd/Fe bimetallic particles: catalytic effects of palladium on hydrodechlorination. Appl Catal B Environ 2007;77:110–16.
[6] He F, Zhao D. Manipulating the size and dispersibility of zerovalent iron nanoparticles by use of carboxymethyl cellulose stabilizers. Environ Sci Technol 2007;41:6216–21.
[7] He F, Zhao D. Preparation and characterization of a new class of starch-stabilized bimetallic nanoparticles for degradation of chlorinated hydrocarbons in water. Environ Sci Technol 2005;39:3314–20.
[8] Wang C, Zhang W. Synthesizing nanoscale iron particles for rapid and complete dechlorination of TCE and PCBs. Environ Sci Technol 1997;31:2154–6.
[9] Freyria FS, Bonelli B, Sethi R, Armandi M, Belluso E, Garrone E. Reactions of Acid Orange 7 with iron nanoparticles in aqueous solutions. J Phys Chem C 2011;115:24143–52.
[10] Shu H, Chang M, Chen C, Chen P. Using resin supported nano zero-valent iron particles for decoloration of Acid Blue 113 azo dye solution. J Hazard Mater 2010;184:499–505.
[11] Fan J, Guo Y, Wang J, Fan M. Rapid decolorization of azo dye methyl orange in aqueous solution by nanoscale zerovalent iron particles. J Hazard Mater 2009;166:904–10.
[12] Xiao S, Shen M, Guo R, Wang S, Shi X. Immobilization of zerovalent iron nanoparticles into electrospun polymer nanofibers: synthesis, characterization, and potential environmental applications. J Phys Chem C 2009;113:18062–8.
[13] Bokare AD, Chikate RC, Rode CV, Paknikar KM. Iron-nickel bimetallic nanoparticles for reductive degradation of azo dye Orange G in aqueous solution. Appl Catal B Environ 2008;79:270–8.
[14] Fang Z, Qiu X, Huang R, Qiu X, Li M. Removal of chromium in electroplating wastewater by nanoscale zero-valent metal with synergistic effect of reduction and immobilization. Desalination 2011;280:224–31.
[15] Kanel SR, Grenèche J, Choi H. Arsenic(V) removal from groundwater using nano scale zero-valent iron as a colloidal reactive barrier material. Environ Sci Technol 2006;40:2045–50.
[16] Kanel SR, Manning B, Charlet L, Choi H. Removal of arsenic(III) from groundwater by nanoscale zero-valent iron. Environ Sci Technol 2005;39:1291–8.
[17] Ponder SM, Darab JG, Mallouk TE. Remediation of Cr(VI) and Pb(II) aqueous solutions using supported, nanoscale zero-valent iron. Environ Sci Technol 2000;34:2564–9.
[18] Qiu X, Fang Z, Yan X, Gu F, Jiang F. Emergency remediation of simulated chromium (VI)-polluted river by nanoscale zero-valent iron: laboratory study and numerical simulation. Chem Eng J 2012;193-194:358–65.
[19] Wang Y, Fang Z, Liang B, Eric Tsang P. Remediation of hexavalent chromium contaminated soil by stabilized nanoscale zero-valent iron prepared from steel pickling waste liquor. Chem Eng J 2014;247:283–90.
[20] Jiang Z, Zhang S, Pan B, Wang W, Wang X, Lv L, et al. A fabrication strategy for nanosized zero valent iron (nZVI)–polymeric anion exchanger composites with tunable structure for nitrate reduction. J Hazard Mater 2012;233-234:1–6.
[21] Jiang Z, Lv L, Zhang W, Du Q, Pan B, Yang L, et al. Nitrate reduction using nanosized zero-valent iron supported by polystyrene resins: role of surface functional groups. Water Res 2011;45:2191–8.
[22] Sohn K, Kang SW, Ahn S, Woo M, Yang S. Fe(0) nanoparticles for nitrate reduction: stability, reactivity, and transformation. Environ Sci Technol 2006;40:5514–19.
[23] Yang GCC, Lee H. Chemical reduction of nitrate by nanosized iron: kinetics and pathways. Water Res 2005;39:884–94.
[24] Liu Y, Majetich SA, Tilton RD, Sholl DS, Lowry GV. TCE dechlorination rates, pathways, and efficiency of nanoscale iron particles with different properties. Environ Sci Technol 2005;39:1338–45.
[25] Kadu BS, Sathe YD, Ingle AB, Chikate RC, Patil KR, Rode CV. Efficiency and recycling capability of montmorillonite supported Fe–Ni bimetallic nanocomposites towards hexavalent chromium remediation. Appl Catal B Environ 2011;104:407–14.
[26] Fang Z, Qiu X, Chen J, Qiu X. Debromination of Polybrominated diphenyl ethers by Ni/Fe bimetallic nanoparticles: influencing factors, kinetics and mechanism. J Hazard Mater 2011;185:958–69.
[27] Xie Y, Fang Z, Cheng W, Pokeung Eric Tsang, Dongye Zhao. Remediation of polybrominated diphenyl ethers in soil using Ni/Fe bimetallic nanoparticles: Influencing factors, kinetics and mechanism. Sci Total Environ 2014;485-486:363–70.
[28] Zhang W, Wang C, Lien H. Treatment of chlorinated organic contaminants with nanoscale bimetallic particles. Catal Today 1998;40:387–95.
[29] Chun CL, Baer DR, Matson DW, Amonette JE, Penn RL. Characterization and reactivity of iron nanoparticles prepared with added Cu, Pd, and Ni. Environ Sci Technol 2010;44:5079–85.
[30] Xu J, Bhattacharyya D. Membrane-based bimetallic nanoparticles for environmental remediation: synthesis and reactive properties. Environ Progr 2005;24:358–66.
[31] Zhu BW, Lim TT, Feng J. Influences of amphiphiles on dechlorination of a trichlorobenzene by nanoscale Pd/Fe: adsorption, reaction kinetics, and interfacial interactions. Environ Sci Technol 2008;42:4513–19.
[32] He F, Zhao D. Preparation and characterization of a new class of starch-stabilized bimetallic nanoparticles for degradation of chlorinated hydrocarbons in water. Environ Sci Technol 2005;39:3314–20.
[33] He F, Zhao D, Liu J, Roberts CB. Stabilization of Fe–Pd nanoparticles with sodium carboxymethyl cellulose for enhanced transport and dechlorination of trichloroethylene in soil and groundwater. Ind Eng Chem Res 2007;46:29–34.
[34] Tiraferri A, Chen KL, Sethi R, Elimelech M. Reduced aggregation and sedimentation of zero-valent iron nanoparticles in the presence of guar gum. J Colloid Interf Sci 2008;324:71–9.
[35] Lin Y, Tseng H, Wey M, Lin M. Characteristics, morphology, and stabilization mechanism of PAA250K-stabilized bimetal nanoparticles. Colloid Surface A: Phys Eng Aspects 2009;349:137–44.
[36] Pera-Titus M, Garcıá-Molina V, Baños MA, Giménez J, Esplugas S. Degradation of chlorophenols by means of advanced oxidation processes: a general review. Appl Catal B Environ 2004;47:219–56.
[37] Abazari R, Heshmatpour F, Balalaie S. Pt/Pd/Fe trimetallic nanoparticle produced via reverse micelle technique: synthesis, characterization, and its use as an efficient catalyst for reductive hydrodehalogenation of aryl and aliphatic halides under mild conditions. ACS Catal 2013;3:139–49.
[38] Xia Z, Liu H, Wang S, Meng Z, Ren N. Preparation and dechlorination of a poly(vinylidene difluoride)-grafted acrylic acid film immobilized with Pd/Fe bimetallic nanoparticles for monochloroacetic acid. Chem Eng J 2012;200-202:214–23.
[39] Wang X, Chen C, Liu H, Ma J. Preparation and characterization of PAA/PVDF membrane-immobilized Pd/Fe nanoparticles for dechlorination of trichloroacetic acid. Water Res 2008;42:4656–64.
[40] Zhou T, Li Y, Lim TT. Catalytic hydrodechlorination of chlorophenols by Pd/Fe nanoparticles: comparisons with other bimetallic systems, kinetics and mechanism. Sep Purif Technol 2010;76:206–14.
[41] Chen C, Wang X, Chang Y, Liu H. Dechlorination of disinfection by-product monochloroacetic acid in drinking water by nanoscale palladized iron bimetallic particle. J Environ Sci 2008;20:945–51.
[42] Parshetti GK, Doong R. Dechlorination of chlorinated hydrocarbons by bimetallic Ni/Fe immobilized on polyethylene glycol-grafted microfiltration membranes under anoxic conditions. Chemosphere 2012;86:392–9.
[43] Wang X, Zhu M, Liu H, Ma J, Li F. Modification of Pd–Fe nanoparticles for catalytic dechlorination of 2,4-dichlorophenol. Sci Total Environ 2013;449:157–67.
[44] Wang X, Chen C, Liu H, Ma J. Characterization and evaluation of catalytic dechlorination activity of Pd/Fe bimetallic nanoparticles. Ind Eng Chem Res 2008;47:8645–51.
[45] Su J, Lin S, Chen Z, Megharaj M, Naidu R. Dechlorination of p-chlorophenol from aqueous solution using bentonite supported Fe/Pd nanoparticles: synthesis, characterization and kinetics. Desalination 2011;280:167–73.